Proceedings of the workshop held at
The Ohio State University

RELATIVISTIC NUCLEAR MANY-BODY PHYSICS

The Ohio State University
June 6-9, 1988

Editors
B.C. Clark
R.J. Perry
The Ohio State University
J.P. Vary
The Ohio State University
and
Iowa State University

World Scientific
Singapore • New Jersey • London • Hong Kong

RELATIVISTIC DYNAMICS IN POLARIZED PROTON SCATTERING FROM POLARIZED ^{13}C

L. Ray
Department of Physics, University of Texas at Austin
Austin, Texas 78712

ABSTRACT

Elastic scattering and charge exchange reactions for polarized proton scattering from polarized ^{13}C are studied using the relativistic distorted wave impulse approximation. Sensitivities of predicted observables to relativistic effects in the nuclear wave function and the Lorentz form of the effective interaction are discussed. The results suggest that it may be possible in this way to obtain new information concerning relativistic dynamics in nuclear structure and scattering processes

1. INTRODUCTION

Polarization phenomenon in intermediate energy proton-nucleus (pA) scattering has been a very rewarding area of research thanks to the realization some five years ago[1] of the importance of relativistic virtual pair effects in the elastic scattering process. Since then the nuclear physics theoretical community has responded with a proliferation of work in this area. We should be encouraged to continue pursuing investigations involving polarization phenomena in medium energy nucleon scattering with an aim towards further elucidation of relativistic dynamics in nuclear many body systems.

In this talk I will discuss the possibilities for continued investigation of relativistic aspects of nuclear reactions and nuclear structure based on studies of medium energy polarized proton scattering and charge exchange reactions from odd target nuclei, which I will also assume to be polarized. Scattering data from odd nuclear targets are sparse at medium energies while polarized target data (other than deuterium) at these energies are nonexistent. A large experimental program to provide proton scattering data from polarized nuclear targets is currently underway at LAMPF.[2,3] In the meantime it is beneficial to both the experimentalists in deciding what to measure and to theorists in evaluating the different models, to investigate the predicted model sensitivities in the elastic and charge exchange channels to the various aspects of relativistic dynamics contained in the current relativistic models of nuclear scattering and structure.

In this presentation I will consider the specific case of elastic scattering of intermediate energy polarized protons from polarized ^{13}C within the framework of the relativistic distorted wave Born approximation (DWBA) using the relativistic impulse approximation

(RIA) to describe the projectile – target nucleon interaction.[1-4-9] Sensitivities are calculated and discussed for the elastic scattering observables with respect to (1) the lower component of the $1p_{1/2}$ valence nucleon wave function, (2) the Lorentz form of the two-body interaction [e.g. pseudoscalar (PS) versus pseudovector (PV) forms], (3) contributions of the even-even core to the isoscalar three-vector current and (4) the individual contributions of the separate Lorentz terms in the two-body interaction.

Following this the same model will be applied to $^{13}C(p,n)$ charge exchange.[8-10] The fact that this reaction is dominated by the large, one-pion exchange component of the effective nucleon-nucleon (NN) interaction makes it an ideal laboratory for studying relativistic aspects of the NN interaction, such as the pseudoscalar versus pseudovector ambiguity.

2 THEORETICAL MODEL

The 500 MeV $\vec{p} + {}^{13}\vec{C}$ elastic scattering observables were calculated using the relativistic impulse approximation for the beam proton – target nucleon interaction,[1-11] a four component, independent particle model for the relativistic target wave function,[12] and the relativistic distorted wave Born approximation for the valence nucleon ($1p_{1/2}$) portion of the $p + {}^{13}C$ elastic scattering amplitude.[7] The core contribution to the scattering amplitude is handled completely within the usual RIA model.[1-4] The first-order RIA potential is given by

$$U^{opt}_{\mu',\mu}(\vec{r}) = U^{core}(\vec{r})\delta_{\mu\mu'} + U^{sp}_{\mu',\mu}(\vec{r}) \tag{1a}$$

where

$$U^{sp}_{\mu',\mu}(\vec{r}) = \int d^3r'\, \bar{u}_{n_b\ell_bj_b\mu'}(\vec{r}')\, t_{pn}(|\vec{r}-\vec{r}'|)\, u_{n_b\ell_bj_b\mu}(\vec{r}'), \tag{1b}$$

where U^{core} is the optical potential for the $J^\pi = 0^+$ 12 nucleon core, $u(\vec{r})$ is the $1p_{1/2}$ valence nucleon wave function and t_{pn} is the projectile (proton) – target valence neutron interaction operator[1-11] [(0) denotes the projectile, (1) the target nucleon].

$$t_{01} = F_S + F_P\,\gamma_0^5\gamma_1^5 + F_V\,\gamma_0^\mu\gamma_{1\mu} + F_A\,\gamma_0^5\gamma_0^\mu\gamma_1^5\gamma_{1\mu} + F_T\,\sigma_0^{\mu\nu}\sigma_{1\mu\nu}. \tag{2}$$

The $1p_{1/2}$ valence nucleon wave function is expressed as

$$u_{n_b\ell_bj_b\mu}(\vec{r}) = \begin{pmatrix} \varphi_{\ell_bj_b}(r)\, Y_{\ell_bj_b\mu}(\hat{r}) \\ i\lambda_{\ell_bj_b}(r)\, Y_{-\bar{\ell}_bj_b\mu}(\hat{r}) \end{pmatrix}, \tag{3}$$

where $Y_{\ell j\mu}(\hat{r})$ is the spin-angle function and $\bar{\ell}_b = \ell_b \pm 1$ if $j_b = \ell_b \pm 1/2$.

In the relativistic distorted wave Born approximation the p + A elastic scattering amplitude is (suppressing spin labels)

$$f = f^{core}\delta_{\mu',\mu} - \frac{m}{2\pi(\hbar c)^2}\langle\chi_c^{(-)}|U^{sp}_{\mu',\mu}|\chi_c^{(+)}\rangle, \tag{4}$$

where f^{core} is the exact scattering amplitude due to U^{core}, m is the proton mass, and χ_c is the relativistic distorted wave function for the proton + 12-nucleon core.

Substituting the partial wave expansions for χ_c, the multipole expansion for t_{pn},[6] and the valence neutron wave function into Eqs. (1b) and (4) yields the partial wave expansion for the $p + {}^{13}C$ elastic scattering amplitude given in Ref. 6. The resulting expression depends on sums of radial integrals containing the radial distorted wave functions and the bound state form factors $F^S_{pnn'}(r)$ which are defined by

$$F^S_{pnn'}(r) = \int_0^\infty r'^2dr'\, T^S_{np}(r,r')\, Z^{nn'}_{\ell_bj_b}(r') \tag{5}$$

where n, S and p denote the Lorentz component, spin dependence and multipole of the NN interaction, respectively.[6] The radial valence wave functions are contained in the quantity $Z(r')$.[6] The label n' accounts for upper and lower component contributions of the valence wave function. A listing of the relevant multipoles, spin and total angular momentum quantum numbers for each component of the NN interaction, along with the corresponding bound state wave function information required in evaluating Eq. (5) is given in Table I.

To include the pseudovector form rather than the PS, the second term in Eq. (2), $F_P\gamma_0^5\gamma_1^5$, is replaced with[13-14] $F_{PV}\gamma_0^5\not{q}\gamma_0^5\not{q}/(4m^2)$ where $\not{q} \equiv q^\mu\gamma_\mu$, q^μ is the 4-momentum transfer, and $F_{PV} = F_P$ using properties of the free particle Dirac equation. The $S = 0$, $n' = 3$ bound state form factor $F^S_{pnn'}(r)$ in Eq. (5) is therefore replaced with

TABLE I

Angular momentum quantum numbers[a] and valence nucleon wave function information for the $p_{1/2} \rightarrow p_{1/2}$ transition.

n	Force Description	S	p	J	Proportional Valence Nucleon Structure
1	scalar	0	0	0	$\|\varphi\|^2 - \|\lambda\|^2$
2	time-like vector	0	0	0	$\|\varphi\|^2 + \|\lambda\|^2$
3	pseudoscalar	0	1	1	$\varphi\lambda$
4	time-like axial vector	0	1	1	(vanishes)
1	tensor_{11}	1	0	1	$\|\varphi\|^2 + 3\|\lambda\|^2$
		1	2	1	$\|\varphi\|^2$
2	axial three-vector	1	0	1	$\|\varphi\|^2 - 3\|\lambda\|^2$
		1	2	1	$\|\varphi\|^2$
3	tensor_{01}	1	1	0	$\varphi\lambda$
		1	1	1	(vanishes)
4	three-vector	1	1	0	(vanishes)
		1	1	1	$\varphi\lambda$

[a] J is the total angular momentum transfer for the target nucleon.

$$F^0_{p3n''}(r) = \left(1+\frac{U_S^{core}(r)}{m}\right)\int_0^\infty r'^2 dr' T^0_{3p}(r,r') Z^{3n''}_{i_b j_b}(r')\left(1+\frac{U_S(r')}{m}\right). \qquad (6)$$

where $U_S^{core}(r)$ and $U_S(r')$ are the scalar parts of the core optical potential and single particle binding potential, respectively.

A longstanding failure of relativistic nuclear structure models has been the large overestimate of the isoscalar magnetic moments of odd nuclei[15] due to enhancement of the lower component of the relativistic wave function of the odd nucleon (due to the strong scalar and vector binding potentials). This problem has been studied by Furnstahl and Serot[16] and by McNeil et al.[17] for infinite nuclear matter. Both show that the isoscalar three-vector current of the odd A target (even-even core plus one particle) can be represented by an effective single particle valence nucleon three-vector current in which enhancement of the lower component of the valence nucleon is suppressed to the weak binding potential value (so-called "nonrelativistic" limit). Core response effects for the isoscalar three vector current at non-zero momentum transfer in finite nuclei have also been studied recently.[18] For the present sensitivity study, a simple model is assumed in which the isoscalar portion of $F^1_{p4n''}(r)$ in Eq (5) is computed assuming the weak, relativistic binding potential (WRBP) limit for the lower component obtained from solution of the bound state Dirac equation with vanishing binding potentials, and is given by

$$\lambda^{WRBP}_{n_b l_b j_b}(r) = \frac{\hbar c}{2m-\varepsilon_{n_b l_b j_b}}\left(\frac{d}{dr} - \frac{\langle\vec{\sigma}\cdot\vec{l}_b\rangle}{r}\right)\varphi_{n_b l_b j_b}(r), \qquad (7)$$

where ε is the valence nucleon binding energy. The remaining form factors and the isovector portion of $F^1_{p4n''}(r)$ are computed as before using a relativistic $\lambda(r)$.

The distorted waves and the core contribution to the full scattering amplitude were computed as explained in Ref. 4 for $J^\pi = 0^+$ targets using the SP82 NN phase shift solution of Arndt,[19] the empirical ^{12}C charge density,[20] empirical values for the neutron vector density,[4] and relativistic mean field theoretical (RMFT) values[12] for the scalar densities. In all of the calculations presented here the core neutron vector density was adjusted (only the surface radius and diffuseness) to improve the overall agreement (not necessarily to obtain a perfect fit) with the preliminary $p + {}^{12}C$ differential cross section data.[21]

The RMFT $1p_{1/2}$ single particle wave function was assumed for φ and λ. In addition the WRBP $\lambda(r)$ of Eq. (7) was used along with the single particle Dirac equation bound state form given by

$$\lambda^{RSPD}_{nlj}(r) = \frac{\hbar c}{2m - \epsilon_{nlj} + U_S(r) - U_V(r)} \left(\frac{d}{dr} - \frac{\langle \vec{\sigma}\cdot\vec{l}\rangle}{r}\right) \varphi_{nlj}(r). \quad (8)$$

which was obtained from solution of the Dirac equation where $U_S(r)$ and $U_V(r)$ are single particle binding potentials.[22] The different models for $\lambda_{1p_{1/2}}$ are shown in Fig. 1.

3. p + ^{13}C ELASTIC SCATTERING RESULTS

Preliminary data[21] for 500 MeV $\vec{p}$ + ^{12}C and ^{13}C(unpolarized) elastic scattering and the predictions of the standard RIA model (i.e., RMFT wave functions for the valence neutron, PS interaction form, no core quenching of the isoscalar, three-vector current) are compared in Figs. 2 - 5. The RIA model provides a qualitative description of these data, being particularly good for the cross sections, but displaying too much structure for D_{SL}. The notation for the D_{ij} measurements is such that subscripts (i) and (j) refer to the initial and final laboratory proton polarization directions, respectively, where $\hat{N}$, $\hat{S}$, and $\hat{L}$ are normal to the scattering plane, perpendicular to the particle momentum and in the scattering plane, and parallel to the particle momentum, respectively. In Fig. 4 the ^{13}C - ^{12}C experimental and RIA model differences are shown for the differential cross sections and analyzing powers. The differences in the predictions are roughly half due to kinematics and half due to the extra interaction with the 13th nucleon. The experimental differences are well described by the standard RIA model. For these unpolarized target observables little sensitivity to different prescriptions for $\lambda_{1p1/2}$ exists and they are also insensitive to the choice of pseudoscalar or pseudovector coupling, quenching of the isoscalar three-vector current, and parts of the NN interaction other than the scalar and time-like vector terms. Nonetheless, careful analyses of such data are required in order to determine the core scattering amplitude. These results show that a successful description of the unpolarized ^{13}C observables primarily requires a realistic treatment of the 12-nucleon core portion of the scattering amplitude.

Preliminary data for p + ^{13}C D_{NN} are shown in Fig. 5 along with several relativistic model predictions, the solid curve representing the standard RIA prediction. The remaining calculations are discussed in the following. The departure of D_{NN} from unity indicates the presence of total angular momentum transfer J = 1 contributions to the elastic scattering channel. These arise from the valence neutron scattering amplitude through the J = 1 components (primarily the pseudoscalar) of the effective NN interaction (see Table 1).

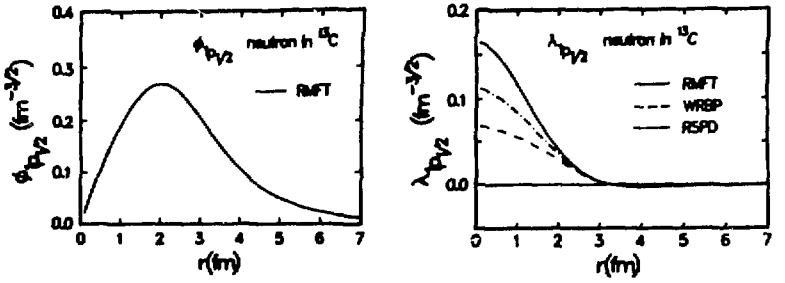

Figure 1 (Refer to text for descriptions of all figures)

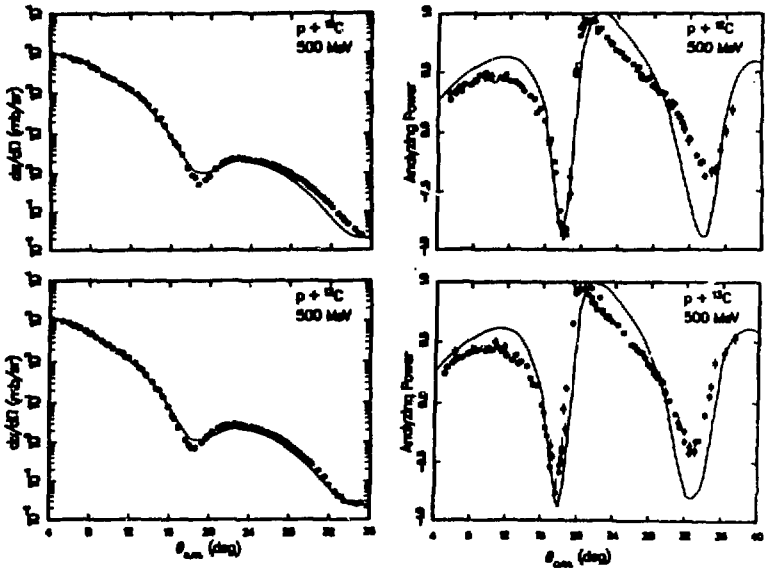

Figure 2

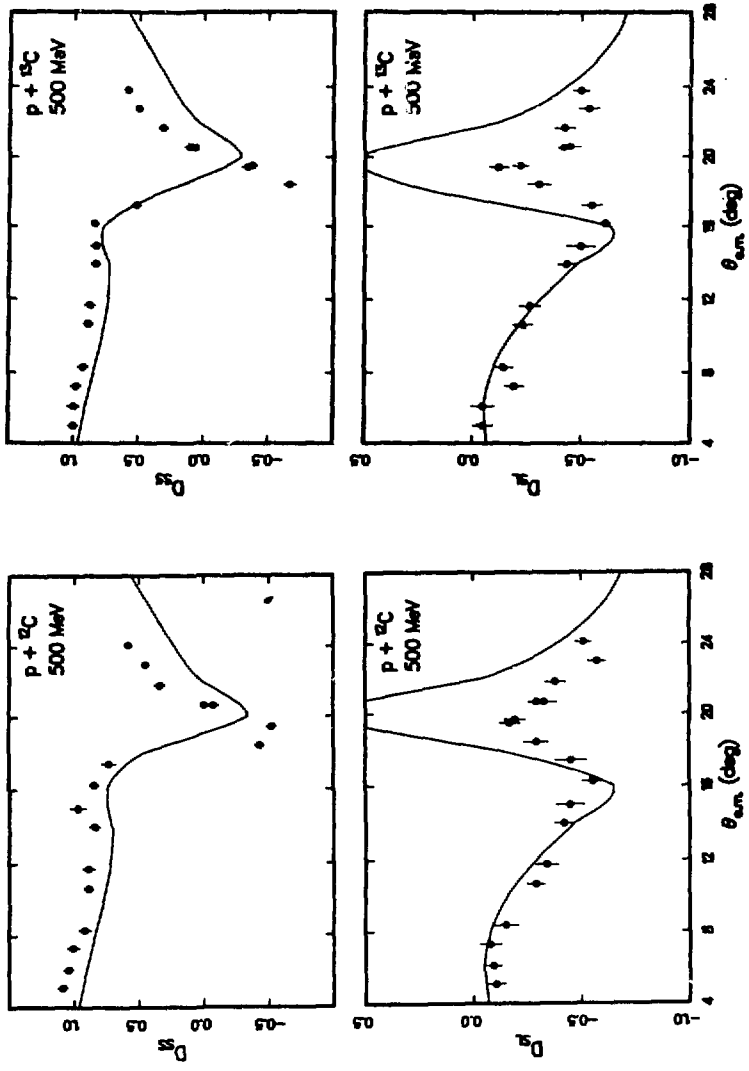

Figure 3

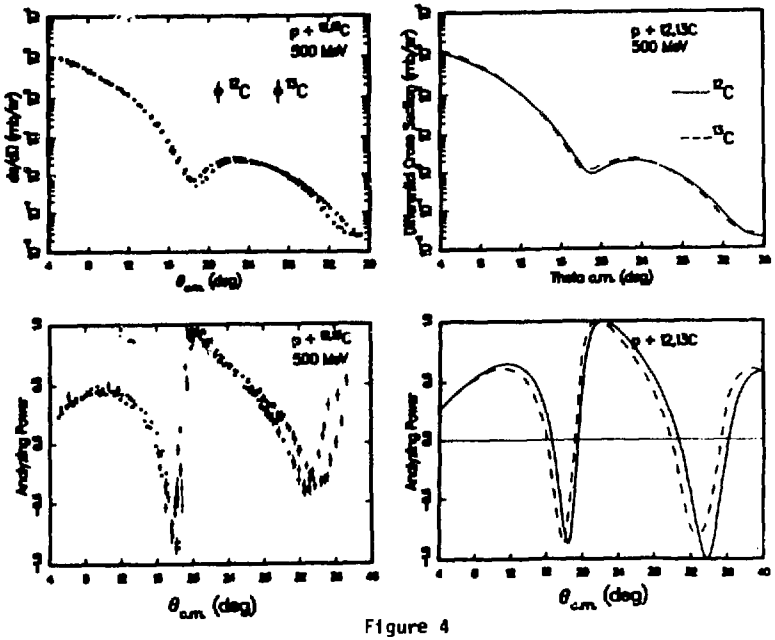

Figure 4

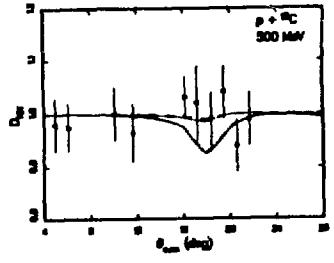

Figure 5

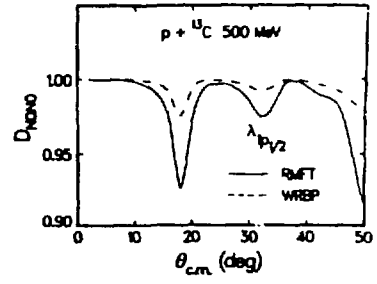

Figure 6

For $p + {}^{13}C$(polarized) elastic scattering the Saclay NN convention for labelling the observables in the pA c.m. was assumed [23]. Observables with spin components in the directions of the c.m. coordinate system [23] $\hat{s}$, $\hat{n}$, and $\hat{l}$ are denoted by subscripts S, N, and L, respectively. In the figures and in the discussion that follows, the observables shown in the figures are c.m. quantities.

Examination of the individual contributions of the various components of the Lorentz invariant NN effective interaction to the $\vec{p} + {}^{13}C$ elastic scattering observables reveals the following. The $\hat{n}$-type polarized target observables are dominated by the space-like, three-vector interaction and are sensitive to relativistic binding potential effects in the lower component $1p_{1/2}$ wave function and to quenching effects in the isoscalar, three-vector current. The $\hat{s}$-type polarized target observables (and also D_{NONO} or D_{NN}) are dominated by the pseudoscalar interaction, are sensitive to $\lambda_{1p1/2}$, and are highly dependent on PS or PV forms.

Moderate sensitivity to $\lambda(r)$ is shown in Fig. 6 for D_{NONO}, and in Figs. 7-8 for selected polarized target observables. The solid curves are standard RIA results where the RMFT value for $\lambda(r)$ is assumed, the dashed curves display the results of similar calculations using $\lambda^{WRBP}(r)$. However, when pseudovector coupling is assumed the model sensitivity to $\lambda(r)$ for D_{NONO} and the $\hat{s}$-type polarized target spin observables is essentially eliminated. For this case the sensitivity to $\lambda(r)$ in the $\hat{n}$-target observables remains, since the pseudoscalar contribution to these observables is negligible. If we additionally adopt both the pseudovector coupling form and the estimated core contribution to the isoscalar three-vector current, the remaining sensitivity to $\lambda(r)$ in the $\hat{n}$-type target observables is also eliminated. Mixing of pseudoscalar and pseudovector interaction contributions, and variations (from that assumed here) in the core contribution to the effective isoscalar three-vector current at finite momentum transfer for finite nuclei might restore some model sensitivity to $\lambda(r)$.

Model sensitivity to pseudovector versus pseudoscalar coupling is shown in Fig. 9 for D_{NONO}, A_{OOLS}, and A_{OOSS}, where the solid (dashed) curves correspond to pseudoscalar (pseudovector) coupling and the relativistic, single particle bound state wave function of Eq. (8) is assumed for $\lambda(r)$. Considerable sensitivity to the choice of Lorentz form is evident in each case shown.

A summary of the model predictions for D_{NONO} and several $\hat{n}$- and $\hat{s}$-target observables for $\vec{p} + {}^{13}C$ at 500 MeV is exhibited in Figs. 5 and 10. The solid curves are results from the standard RIA calculation (i.e., RMFT $\varphi(r)$ and $\lambda(r)$, PS coupling). Predictions obtained assuming pseudovector coupling with RMFT $\varphi(r)$ and $\lambda(r)$ from Eq. (8) are indicated by the dashed curves. Results using PS coupling and the quenched isoscalar three-vector current (RMFT values for φ and λ) are shown by the dashed-dotted lines. Finally, the model results obtained assuming both pseudovector coupling and quenching of the isoscalar three-vector current (RMFT φ and λ of Eq. (8)) are given by the dotted curves. The results in Figs. 5 and 6 for D_{NN} suggest a preference either for PV coupling or the PS form with $\lambda^{WRPB}(r)$. Comparison of these predictions with the forthcoming polarized ^{13}C

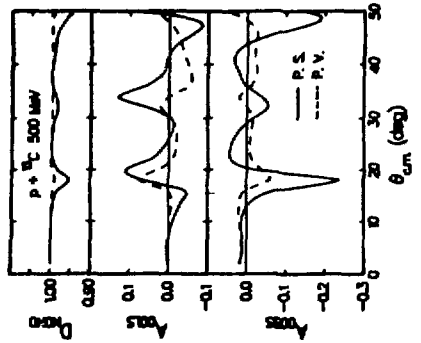

Figure 9

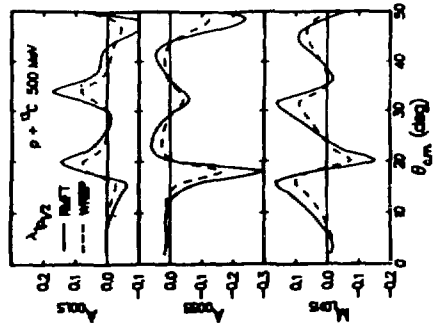

Figure 8

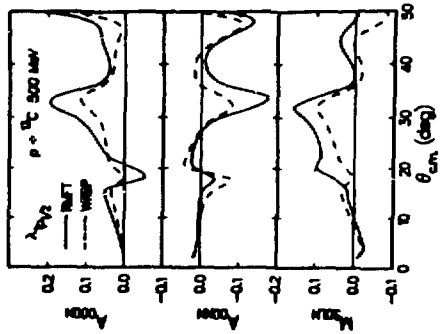

Figure 7

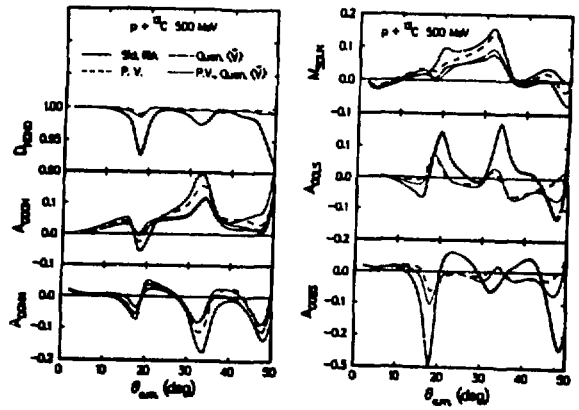

Figure 10

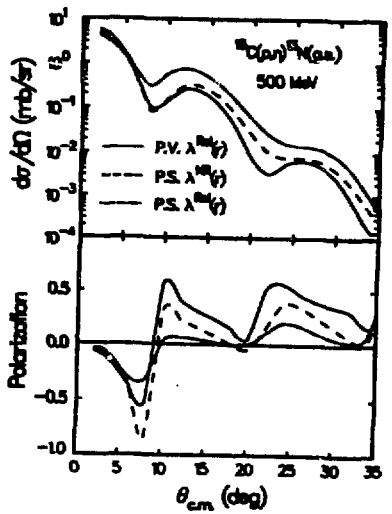

Figure 11

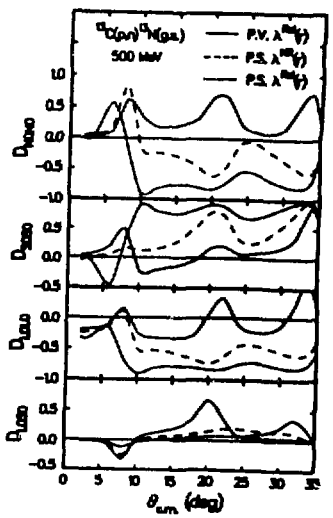

Figure 12

data will be very exciting and will undoubtedly challenge the underlying theoretical models and assumptions.

4 500 MeV ^{13}C(p,n) CHARGE EXCHANGE RESULTS

Because of the dominant strength of the PS invariant and given the importance of the PS - PV ambiguity, studies which focus on this specific component of the NN interaction would clearly be worthwhile. Because the PS component of the NN interaction derives primarily from one-pion exchange it is strongly isovector and involves angular momentum transfer. Gamow-Teller (GT) transitions therefore provide the suitable candidate for such studies. Examinations of relativistic effects in predicted GT transitions in ^{12}C(p,p') have been presented already.[24] Here and in Refs. 8 and 10 the sensitivity of (p,n) reaction observables to PS versus PV forms is evaluated using the RIA *DWBA* model discussed in the preceding. The particular case chosen is 500 MeV ^{13}C(p,n)^{13}N leading to the isobaric analogue state (IAS) in ^{13}N. This and other (p,n) reactions are currently being measured at the neutron time-of-flight (NTOF) facility at LAMPF.[25]

Each term in the NN relativistic invariant amplitude is assumed to be isospin dependent according to

$$F_j = F_j^0 + F_j^1\, \vec{\tau}_{(1)}\cdot\vec{\tau}_{(2)},\quad j = S,P,V,A,T \qquad (9)$$

where $\vec{\tau}$ is the usual nucleon isospin operator. The charge exchange transition amplitude is evaluated in the RIA - DWBA model exactly as for the case of p + ^{13}C elastic scattering, except that the isovector NN interaction is used and there is no core contribution. For the calculations presented here isospin invariance is assumed for the bound state and distorted wave functions. The charge exchange amplitude contains both $\Delta J^{\pi} = 0^+$ and 1^+ components corresponding to Fermi and Gamow-Teller transitions.

The effects of particle-hole mixing in the predicted ^{13}C(p,n) observables have been estimated[8] and the predicted sensitivities to PS versus PV forms are not expected to be qualitatively altered by configuration mixing in the A = 13 ground state. Improved nuclear structure input will be required before meaningful comparison with future data will be possible.

Predictions for the 500 MeV ^{13}C(p,n)^{13}N(IAS) differential cross section and polarization are shown in Fig. 11. Suppressing the $1p_{1/2}$ lower component in the PS calculation or use of the PV form of the NN amplitude both reduce the overall magnitude of the differential cross section relative to the PS, λ^{RSPD} prediction. The PS calculation assuming λ^{WRBP} is similar to the PV prediction at forward angles less than 20°. Because the PS calculations with λ^{WRBP} for the differential cross section are similar to the PV results at forward angles comparison with differential cross section data alone is insufficient to uniquely distinguish between the two forms for the NN amplitudes.

The polarization displays similar trends in that significant sensitivity to PV versus PS forms (with λ^{RSPD}) is indicated and the PS, λ^{WRBP} prediction (dashed curve) is similar to the PV result.

The spin depolarization observables D_{NONO}, D_{SOSO} and D_{LOLO} shown in Fig. 12 display considerable sensitivity to both the choice of PV versus PS form and to relativistic binding potential effects in the lower component of the valence nucleon wave function (for the PS calculations only). Large, qualitative differences between either of the two PS calculations and the PV prediction are demonstrated for each D_{i0i0} observable. The D_{LOSO} predictions indicate some sensitivity to the PS versus PV form and to the strength of $\lambda(r)$ (for the PS calculations) but are not as dramatic as that displayed by the D_{i0i0} predictions. Similar calculations for polarized target observables do not demonstrate sensitivity to λ or PV versus PS forms which is as dramatic as that provided by the D_{i0i0} observables. The absence of core contributions to the (p,n) transition amplitude permits the PS versus PV effects to become appreciable for the unpolarized target observables,[8-10] unlike the situation for proton elastic scattering from ^{13}C (Ref. 6).

5. SUMMARY AND CONCLUSIONS

The principal results of this study are the following: (1) the unpolarized, odd-target observables (except for D_{NONO}) are primarily sensitive to just the scalar and time-like vector NN interaction contributions of the core, (2) significant sensitivity to relativistic enhancement of $\lambda(r)$ exists for most $\hat{n}$ and $\hat{s}$-target spin observables in the standard RIA model, but this sensitivity disappears when the theoretically motivated PV model with quenched isoscalar three-vector currents is used, (3) sensitivity to PV versus PS coupling is amply demonstrated in D_{NONO} and the $\hat{s}$-target observables, (4) $\hat{n}$-target observables are dominated by the isoscalar three-vector current (space-like vector contribution) and are sensitive to core contributions to such currents, and (5) theoretical spin depolarization predictions. D_{i0i0} for the few hundred MeV proton induced IAS charge exchange reaction from unpolarized ^{13}C are directly sensitive to the PS versus PV form, the predictions remaining distinct regardless of the (reasonable) assumptions made for the valence nucleon lower component wave function. A variety of predictions for several 500 MeV $\vec{p}$ + ^{13}C elastic scattering and charge exchange spin observables were given.

It can be concluded from this work that analyses of intermediate energy polarized proton elastic scattering data from light weight, polarized nuclear targets should, in principle, provide a wealth of new information related to the following: (1) the Lorentz character of the NN effective interaction, (2) spin saturated core contributions to the total isoscalar three-vector current, (3) effective strengths and ranges of various parts of the NN interaction, and (4) possible relativistic binding potential enhancement of the lower component of the valence nucleon wave function. However, when faced with the analysis of actual $\vec{p}$ + ^{13}C elastic scattering and charge exchange data in the future it should be realized that the physics which must be ultimately dealt with is immensely complex, entailing most of the intermediate energy reaction dynamics known to be important and requiring very detailed relativistic and nonrelativistic nuclear structure calculations for a nucleus in a region of the periodic table whose properties are notoriously difficult to understand. Further progress in this theoretical investigation will most likely require, (1) relativistic, coupled channels calculation, (2) sophisticated relativistic NN interaction models based on meson exchange theory, and (3) exchange, correlation, off-shell, and medium effects, etc. We hope that the interesting results obtained in this work will stimulate the theoretical community to address these and other problems.

ACKNOWLEDGEMENTS.

The collaborative efforts of Drs. G. W. Hoffmann, M. L. Barlett, J. D. Lumpe, B. C. Clark, S. Hama, R. L. Mercer, J. R. Shepard, and B. D. Serot are gratefully acknowledged. This research was supported in part by the U. S. Department of Energy.

REFERENCES

1. J. A. McNeil, J. Shepard, and S. J. Wallace, Phys. Rev. Lett. 50, 1439, 1443 (1983), and B. C. Clark, S. Hama, R. L. Mercer, L. Ray, and B. D. Serot, Phys. Rev. Lett. 50, 1644 (1983).
2. See the following Los Alamos Meson Physics Facility (LAMPF) experimental proposals, EXP. 955, spokesmen G. W. Hoffmann, R. L. Ray, M. L. Barlett, and J. J. Jarmer, EXP. 1025, spokesmen G. R. Burleson and D. Dehnhard, and EXP. 1023, spokesmen J. Comfort and G. Kyle.
3. Proceedings of the LAMPF Workshop on Physics with Polarized Nuclear Targets, LAMPF Conference Report LA-10772-C, edited by G. Burleson, W. Gibbs, G. Hoffmann, J. J. Jarmer, and N. Tanaka, Los Alamos National Laboratory (1986).
4. L. Ray and G. W. Hoffmann, Phys. Rev. C31, 538 (1985).
5. L. Ray et al., Phys. Rev. Lett. 56, 2465 (1986).
6. L. Ray et al., Phys. Rev. C37, 1169 (1988).
7. J. R. Shepard, E. Rost, and J. Piekarewicz, Phys. Rev. C30, 1604 (1984).
8. See the article in Ref. 3 by J. Shepard, page 73.
9. See the article in Ref. 3 by L. Ray, page 41.
10. L. Ray and J. R. Shepard, University of Texas preprint (1988).
11. J. A. McNeil, L. Ray, and S. J. Wallace, Phys. Rev. C27, 2123 (1983).
12. C. J. Horowitz and B. D. Serot, Nucl. Phys. A368, 503 (1981). The valence neutron wave function from this work is actually the $1p_{1/2}$ single particle eigenstate of the ^{12}C relativistic Hartree binding potential.
13. C. J. Horowitz, Phys. Rev. C31, 1340 (1985).
14. J. A. Tjon and S. J. Wallace, Phys. Rev. C32, 1667 (1985).
15. L. D. Miller, Ann. Phys. (N. Y.) 91, 40 (1975).
16. R. J. Furnstahl and B. D. Serot, Nucl. Phys. A468, 539 (1987).
17. J. A. McNeil et al., Phys. Rev. C34, 746 (1986).

18. J. R. Shepard, E. Rost, C. Y. Cheung, and J. A. McNeil, University of Colorado preprint NPL-1029 (1987), and J. R. Shepard, private communication.
19. R. A. Arndt, J. S. Hyslop III, and L. D. Roper, Phys. Rev. D35, 128 (1987); and R. A. Arndt et al., Phys. Rev. D28, 97 (1983).
20. I. Sick and J. S. McCarthy, Nucl. Phys. A150, 631 (1970).
21. G. W. Hoffmann et al., in preparation.
22. Two-parameter Fermi function fits to the relativistic Hartree potentials for ^{12}C were used.
23. J. Bystricky, F. Lehar, and P. Winternitz, J. de Phys. 39, 1 (1978).
24. D. A. Sparrow et al., Phys. Rev. Lett. 54, 2207 (1985); and J. Piekarewicz, R. D. Amado, and D. A. Sparrow, Phys. Rev. C32, 949 (1985).
25. G. W. Hoffmann and D. Ciskowski, LAMPF experimental proposal No. 1041, Los Alamos National Laboratory (1988).